

Predicting Partition Coefficients of Short-Chain Chlorinated Paraffin Congeners by Combining COSMO-RS and Fragment Contribution Model Approaches

Satoshi Endo, Jort Hammer*

National Institute for Environmental Studies (NIES), Center for Health and Environmental Risk Research, Onogawa 16-2, 305-8506 Tsukuba, Ibaraki, Japan

*Corresponding author

Satoshi Endo, Phone/Fax: ++81-29-850-2695, endo.satoshi@nies.go.jp

Abstract

Chlorinated paraffins (CPs) are highly complex mixtures of polychlorinated *n*-alkanes with differing chain lengths and chlorination patterns. Knowledge on physicochemical properties of individual congeners is limited but needed to understand their environmental fate and potential risks. This work combines a sophisticated but time-demanding quantum chemically based method COSMO-RS and a fast-running fragment contribution approach to establish models to predict partition coefficients of a large number of short-chain chlorinated paraffin (SCCP) congeners. Molecular fragments of a length of up to C₄ in CP molecules were counted and used as explanatory variables to develop linear regression models for predicting COSMO-RS-calculated values. The resulting models can quickly provide COSMO-RS predictions for octanol–water (K_{ow}), air–water (K_{aw}), and octanol–air (K_{oa}) partition coefficients of SCCP congeners with an accuracy of 0.1–0.3 log units root mean squared errors (RMSE). The model predictions for K_{ow} agree with experimental values for individual constitutional isomers within 1 log unit. The ranges of partition coefficients for each SCCP congener group were computed, which successfully reproduced experimental log K_{ow} ranges of industrial CP mixtures. As an application of the developed approach, the predicted K_{aw} and K_{oa} were plotted to evaluate the bioaccumulation potential of each SCCP congener group.

31 Introduction

32 Chlorinated paraffins (CPs) are highly complex mixtures of polychlorinated *n*-alkanes with
33 variable numbers of C and Cl atoms. Short-chain chlorinated paraffins (SCCPs, C₁₀–C₁₃) are considered
34 persistent, bioaccumulative, and toxic and thus have been regulated under the Stockholm Convention
35 since 2017.¹ Medium-chain CPs (MCCPs, C₁₄–C₁₇) and long-chain CPs (LCCPs, C₁₈+) are not under
36 regulation at the present time, although concerns have been raised, particularly for MCCPs, whether
37 regulation should be implemented for these longer CPs.² CP products contain a considerable number
38 of congeners with different molecular structures. To date, analytical methods are not available that
39 fully resolve individual congeners from mixtures.³ Environmental assessments for bulk CP mixtures
40 often use average properties. However, once diluted in the environment, each congener behaves
41 individually following its own properties. As has been learned from decades of studies on other
42 halogenated organic pollutants such as polychlorinated dibenzo-*p*-dioxins and polychlorinated
43 biphenyls, environmental behavior and toxicity are often highly congener-specific. Indeed, broad
44 bands of CP signals from chromatographic analysis⁴ suggest that the properties of congeners differ
45 substantially.

46 To address the environmental fate and toxicity of individual CP congeners, their partitioning
47 properties need to be understood. Experimental determination of such properties is only possible for
48 a handful of congeners because the availability of pure analytical standards is currently limited.
49 Computational methods may be the only possibility to provide congener-specific information. Among
50 such prediction models available, empirical fit models may not be useful, as congener-specific
51 experimental data are not sufficiently available to calibrate such models.

52 This study applies the quantum chemically based COSMO-RS theory⁵ to predict partition
53 coefficients of CP congeners. COSMO-RS can predict partition coefficients from the molecular
54 structure alone without any additional empirical parameter. This approach could address partition
55 coefficients of CP congeners with differing structures even including stereoisomers. Previous studies
56 show that COSMO-RS can predict partition coefficients for chemicals of diverse structures (but no
57 CPs) to the accuracy of < 1 log unit root-mean squared errors (RMSE) as compared to experimental
58 data, including chemicals with multifunctional structure.^{6,7} Relative values across chemicals are
59 expected to be even more accurate because systematic errors are canceled.⁸

60 The problem of using COSMO-RS for predicting a large number of chemicals is the
61 computational time needed for the quantum chemical calculation and the conformer selection. For
62 example, it takes several hours to generate COSMO files, necessary to calculate partition coefficients,
63 just for a single (stereo)isomer of C₁₀Cl₁₀ using the supercomputer at the National Institute for
64 Environmental Studies (HPE Apollo 2000, Intel Xeon Gold 6148 CPU, 40 CPU cores per each job). The
65 computational time generally increases with the size of the molecule. Indeed, Glüge et al.⁹ previously
66 applied COSMO-RS to predict partition coefficients of CPs but provided predictions for only 4
67 structures per congener group, which are too few to address the variability of partition coefficients
68 across congeners.

69 To enable the prediction of partition coefficients for hundreds of thousands of CP congeners,
70 this study combines COSMO-RS with a fragment contribution model (FCM). An FCM counts the
71 substructures (fragments) within the molecule and uses the fragment counts as descriptors for
72 regression analysis. Such models have been widely adapted in the predictive model development of
73 environmental properties.¹⁰⁻¹³ FCMs are a linear model that can provide predictions with high speed
74 and low electric energy consumption. In this work, we regress the COSMO-RS-predicted partition
75 coefficients against CP's fragment counts to develop a model for predicting COSMO-RS predictions.
76 Developing a model to predict the values that are output of another model might seem unmeaningful,
77 because such a secondary model can only give less accurate predictions than the original model.
78 However, such an approach is increasingly used in quantum chemistry applications where
79 computational time is a hampering issue.¹⁴ A secondary but fast-running fragment model could be
80 useful particularly for CPs, and possibly other complex mixture components, because 1) experimental
81 data for individual congeners are not available, 2) computation of the original model is too slow to
82 cover the enormous number of congeners, and 3) the chemicals of concern are made up of relatively
83 simple fragments and thus simple FCMs are expected to reproduce the predictions from a more
84 sophisticated model well.

85

86 Methods

87 **Method overview.** COSMO-RS-based FCMs for the log of octanol–water (K_{ow}), air–water
88 (K_{aw}), and octanol–air (K_{oa}) partition coefficients of SCCPs were developed by the following procedure.
89 (1) The respective partition coefficients for a number of CP structures were calculated using the
90 COSMO-RS method to generate training and validation sets. (2) FCMs with different combinations of
91 fragments were calibrated using the training set. (3) Predictive performance of the calibrated FCMs
92 was evaluated with the validation set. (4) Predictions by the FCMs were compared to available
93 experimental data. (5) The FCMs were used to predict randomly generated SCCP congeners (1000
94 each for 52 congener groups) to demonstrate the variations of partition coefficients for SCCPs.

95 The CPs considered in this work are polychlorinated *n*-alkanes (i.e., no branching, no multiple
96 bond). In this article, we refer to individual CP structures with different chain lengths and Cl-
97 substitution patterns as “congeners”. A “congener group” collectively denotes the congeners with the
98 same number of C and Cl atoms (i.e., isomers). Isomers of CPs include stereoisomers that have the
99 same two-dimensional molecular structure but are not superimposable in the three-dimensional
100 space because of the presence of chiral centers.

101 **COSMO-RS.** COSMO-RS calculates the chemical potential of solute in solution from quantum
102 mechanics and statistical thermodynamics calculations and can thereby predict thermodynamic
103 properties including partition coefficients.⁵ For a given stereochemically specific congener, the
104 molecular structure in the SDF format was entered into the COSMOconfX 4.3 software (COSMOlogic),
105 which selected optimal conformers and generated their COSMO files using quantum chemistry
106 program TURBOMOL 7.3 (COSMOlogic). These COSMO files were then used in COSMOthermX 19.0.4

107 (COSMOlogic, parameterization: BP_TZVPD_FINE_19) to calculate K_{ow} , K_{aw} , and K_{oa} at 25°C. Here, we
108 calculated K_{ow} with wet octanol and K_{oa} with dry octanol. Note that the version of COSMOconfX used
109 in this work sometimes returned structures that are stereochemically inconsistent with the original
110 structure in the SDF (i.e., incorrect *R* or *S* configuration). This problem did not occur when we used
111 the Windows version of COSMOconfX, switched off RDKit, and used only Balloon to generate initial
112 candidate conformers.

113 The whole calculation procedure from COSMOconfX to COSMOthermX is consistent,
114 although a slight difference in the calculated partition coefficient sometimes occurs when the initial
115 input structure entered in COSMOconfX is in a different conformational state. We examined the
116 extent of this “random error” using 10 starting conformations each for three arbitrarily chosen C_{10}
117 congeners. The standard deviations for $\log K_{ow}$, $\log K_{aw}$, and $\log K_{oa}$ were on average 0.02, 0.14, and
118 0.12, respectively. These differences may represent the current precision of COSMOtherm predictions
119 for CPs.

120 **Generation of training and validation sets.** In this work, we used “very” short to short-chain
121 CPs (C_5 – C_{10}) as training chemicals because computational time of the COSMOconfX optimization
122 procedure increases with the size of molecule. By opting for short CPs, we were able to generate
123 many congeners for model training. The validation set, in contrast, should comprise congeners that
124 are relevant. We chose C_{10} – C_{13} , thus SCCPs in this work. Calibrating and/or testing models for MCCPs
125 and LCCPs would also be interesting but need much more time for calculations and was thus left for
126 future work.

127 The training set consisted of 815 congeners—all 315 distinct isomers of C_5 CPs and 100
128 randomly generated isomers for each of C_6 to C_{10} CPs. In random generation, 0 to $(2m + 2)$ H atoms
129 of C_m -*n*-alkanes were randomly substituted with Cl atoms without any restriction. Here, all H atoms
130 were considered distinct to also generate stereoisomers. Equivalent structures (i.e., superimposable
131 by rotation) and enantiomers (i.e., mirror images) were removed because they show the identical
132 partition coefficient value in reality, and COSMO-RS should give the same value in theory.
133 Diastereomers, in contrast, can have different partitioning properties and thus are considered distinct
134 congeners. The validation set consists of 120 CP congeners (30 for each of C_{10} to C_{13} CPs) that were
135 also randomly generated. Codes were written in the *R* language¹⁵ to create SMILES strings for all these
136 congeners. SMILES was then converted to SDF format using OpenBabel,¹⁶ which was then fed to
137 COSMOconfX as described above.

138 **Fragment contribution models (FCMs).** Fragments in CP structures were counted using *R*
139 with ChemmineR (3.38.0) and ChemmineOB (1.24.0) packages from Bioconductor.¹⁷ Fragments with
140 differing carbon-chain lengths, namely C_1 , C_2 , C_3 , and C_4 fragments were considered (Table S1 in the
141 Supporting Information, SI). These fragments, respectively, have 7, 19, 64, and 220 types, out of which
142 0, 1, 10, and 67 types describe the diastereomeric patterns. All fragments and their SMARTS queries
143 are given in Table S2. Using these fragments, four levels of models were generated. Level 1 model
144 used only C_1 fragments, and Level 2 model included C_1 and C_2 fragments. Levels 3 and 4 were

145 calibrated with C_1 to C_3 and C_1 to C_4 , respectively. Models were calibrated with least square multiple
146 linear regression (MLR) with fragment counts as explanatory variables and COSMO $_{therm}$ predictions
147 as dependent variables. Since fragment counts are not fully independent and the contributions of
148 some (or many) fragments to the partition coefficient can be insignificant, a forward and backward
149 stepwise algorithm was used to select model variables (i.e., fragments). Akaike's Information Criterion
150 (AIC) was considered the model evaluation metric.¹⁸ Variable selection was first performed for the
151 Level 1 model. Then, the selected C_1 fragments were used as the initial variable set of the variable
152 selection procedure for the Level 2 model, and so forth. To overcome a possible over-fitting problem,
153 partial least squares regression (PLSR) was also performed using the selected Level 4 model fragments.
154 The randomization test method was used to decide on the number of PLS components. All these
155 statistical analyses were performed with *R* using functions such as `lm()`, `step()`, `pls()`, and
156 `selectNcomp()`.

157 **Predictions of partition coefficients for congener groups.** Using the FCMs calibrated with
158 PLSR, $\log K_{ow}$, $\log K_{aw}$, and $\log K_{oa}$ for 1000 randomly generated isomers for each SCCP congener group
159 (C_{10} – C_{13} , Cl_2 – Cl_{14}) were predicted. Two methods were adapted to generate random isomers. In the
160 first method, all H atoms were considered available for Cl substitution at the same likelihood. Second,
161 all H atoms were available, but each C atom was able to carry a maximum of only one Cl atom. In
162 other words, the first method allows double or triple Cl substitution, while the second does not. For
163 the second case, congeners with the number of Cl > the number of C cannot be generated. Also, if Cl
164 = C, then there is only one constitutional isomer (but with many stereoisomers). As for random
165 generation of training and validation sets explained above, all substitution positions along the carbon-
166 chain were considered distinct to account for stereoisomers. Duplications were allowed for random
167 generation of 1000 isomers; this matters the most for $C_{10}Cl_2$ group, which has only 30 constitutional
168 isomers with 46 distinct structural isomers (i.e., 16 constitutional isomers have diastereomers).
169 Duplication occurs increasingly rarely as the number of Cl approaches that of C. For example, 1000
170 random isomers of $C_{10}Cl_{10}$ had only 10 duplications and 14 enantiomer pairs.

171 We are aware that existing studies have shown that Cl substitution patterns are not random
172 in commercial CP mixtures. A recent study suggested that the first, second, and third carbons from
173 an end of the chain and central carbons all have differing likelihood of chlorination.¹⁹ Also, it has been
174 known that chlorination occurs less likely to the neighbors of the carbon that is already chlorinated
175 due to a steric effect,^{20,21} which is also inferred by GC retention measurements for CP mixtures.^{4,22}
176 Nevertheless, in highly chlorinated CP mixtures, dichloro-substituted carbons and trichloromethyl
177 groups have also been identified.^{19,23} Since general rules for positions of Cl for CPs of different lengths
178 and chlorination degree are still under investigation, we opted for the fully random and "one Cl per
179 C" rules to generate congener sets for this work.

180

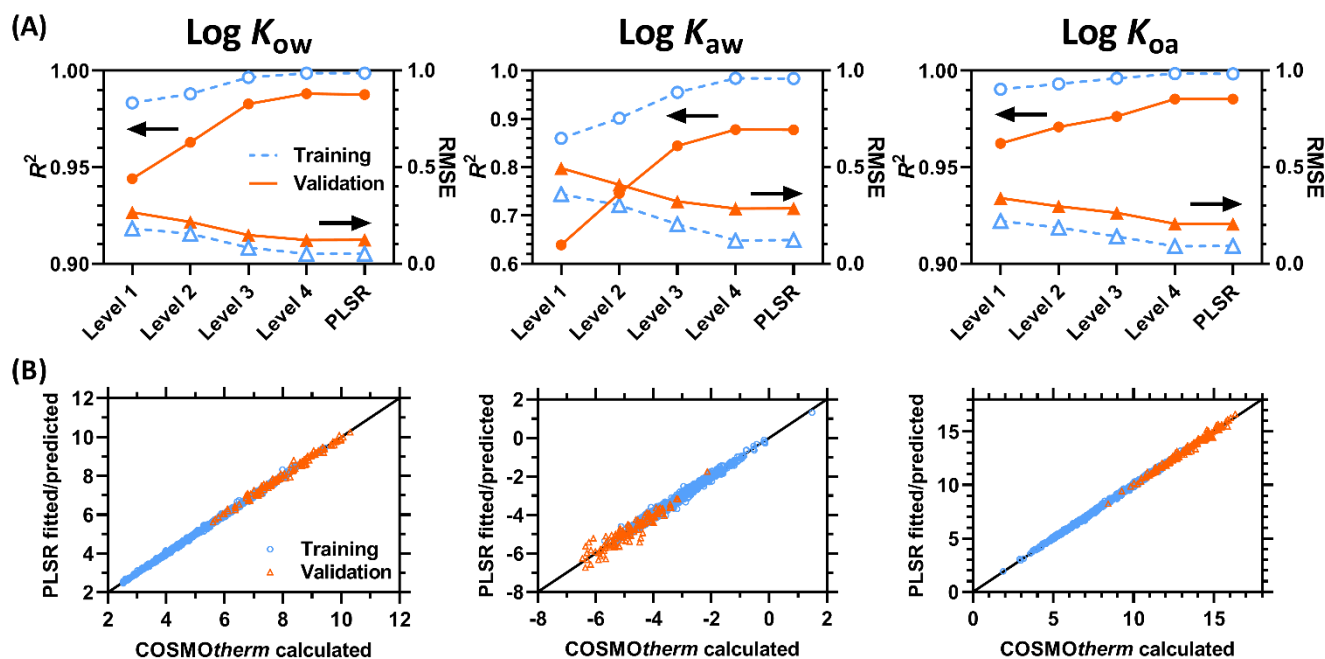
181 Results and discussion

182 **FCM training and validation.** For all of $\log K_{ow}$, $\log K_{aw}$, and $\log K_{oa}$, increasing the number of

183 fragments for MLR from Level 1 to Level 4 models improved the fitting quality, as indicated by R^2 , root
184 mean squared errors (RMSE), and AIC (Figures 1, S1, S2, Table S3). Hence, Level 4 model resulted in
185 the best fit. It is interesting that C_4 fragments do have statistically significant contributions to the
186 partition coefficients, suggesting that the molecular interaction properties of CPs cannot fully be
187 reduced to the shorter fragments, at least in the COSMO-RS calculation. In the variable selection
188 procedure, about half (49-61%) of the total fragments were removed for Level 2 to 4 models. This is
189 not surprising, because many fragments share common substructures and thus are interrelated. PLSR
190 with the Level 4 fragments resulted in a similar fitting quality as compared to the least square MLR,
191 although the PLSR has more restrictions (i.e., a lower degree of freedom) when deriving fitting
192 coefficients. The good fit indicated by low RMSE (0.05, 0.12, and 0.09 for $\log K_{ow}$, $\log K_{aw}$, and $\log K_{oa}$,
193 respectively) with the Level 4 model or its PLSR version show that FCMs can accurately fit
194 COSMO $therm$ calculated values for CPs. These RMSE values are similar to the precision of
195 COSMO $therm$ for CPs mentioned in the Methods section and may thus be considered the best
196 achievable fit. All resulting fitting coefficients are presented in Table S4. We note that some fragments
197 that describe diastereometric structures were also significant.

198 External validation leads to the same conclusions as above. Thus, the Level 4 model showed
199 the best statistics, and the statistics were better in order of $\log K_{ow}$, $\log K_{oa}$, and $\log K_{aw}$. (Figures 1 and
200 S3, Table S3). PLSR and the Level 4 model predicted the validation set equally well. While PLSR
201 typically is considered more robust when the number of variables is large, it was just similar to the
202 least square MLR-based Level 4 model. RMSE was 0.12, 0.29, and 0.21 for $\log K_{ow}$, $\log K_{aw}$, and $\log K_{oa}$,
203 respectively, being 2.2–2.4 times higher than RMSE for fitting. Use of the calibrated FCMs thus causes
204 additional prediction errors of 0.1 to 0.3 RMSE in $\log K$'s of SCCPs, as compared to the direct use of
205 COSMO $therm$.

206



207

208 Figure 1. Statistics of model fitting and validation (A) and comparison of FCM (PLSR)-calculated values
 209 to training and validation data (B). Arrows indicate the axes that the data points refer to. Larger figures
 210 (Figures S1–S3) and a table with statistics for all models (Table S3) are presented in the SI.

211

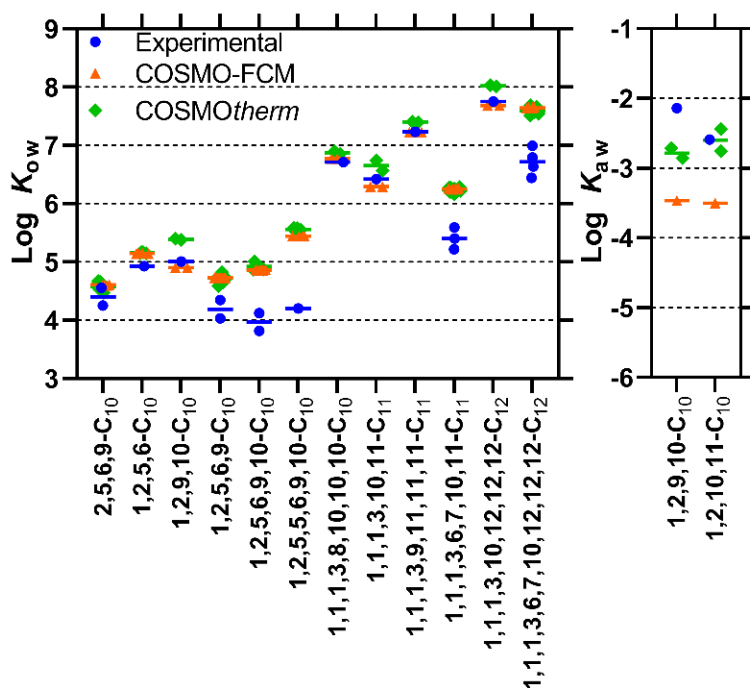
212 **Fragment contributions to $\log K$'s.** The fact that the level 4 model performs the best suggests
 213 that the actual contribution of each C type (e.g., $-\text{CH}_2-$, $-\text{CHCl}-$) to $\log K$'s depends on its neighboring
 214 structure. Nevertheless, lower level models may also be useful to illustrate the average contributions
 215 of the C types to $\log K$'s. For instance, the Level 1 model (with only C_1 fragments) shows that the
 216 fragment contributions to $\log K_{ow}$ and $\log K_{oa}$ are fairly systematic (Figure S4): The $-\text{CH}_2-$ increment
 217 increases $\log K_{ow}$ and $\log K_{oa}$, while substituting H of $-\text{CH}_2-$ or CH_3- with Cl also increases $\log K_{ow}$
 218 and $\log K_{oa}$. In contrast, the fragment contributions to $\log K_{aw}$ are irregular. Substituting one H in $-\text{CH}_2-$
 219 with Cl to form $-\text{CHCl}-$ decreases $\log K_{aw}$, but further substitution to $-\text{CCl}_2-$ would not change $\log K_{aw}$.
 220 Similarly, Cl-substitution of CH_3- to $\text{CH}_2\text{Cl}-$ decreases $\log K_{aw}$, but further substitution to CHCl_2- has no
 221 influence, and that to CCl_3- even increases $\log K_{aw}$.

222

223 **Comparison to experimental data.** There are some experimentally determined $\log K_{ow}$ and
 224 $\log K_{aw}$ for specific constitutional isomers in the literature. The predictions by the FCM (PLSR-
 225 calibrated) agree with the literature data for $\log K_{ow}$ within 1 log unit difference (Figure 2). The FCM
 226 tends to overpredict $\log K_{ow}$ of CP congeners with five or more chlorinated C atoms. The predictions
 227 by the original COSMOtherm deviate from the experimental data to a similar extent. Thus, the
 228 observed overpredictions for some $\log K_{ow}$ data should be related to the inaccuracy in the original
 229 COSMOtherm calculations or due to experimental errors. The cited experimental data were derived
 230 from HPLC retention measurements using 10 hydrophobic aromatic compounds as calibration

231 compounds. While this is a standard approach, the resulting K_{ow} may not be as accurate for aliphatic
232 chemicals with appreciable polarity like CPs as for hydrophobic aromatic compounds.

233 The two congener-specific experimental $\log K_{aw}$ are underpredicted by the FCM by 1–1.5 log
234 units. The original COSMOtherm predictions agree better with the experimental data in this case. As
235 Figure 2 shows, the predictions for K_{aw} by FCM and COSMOtherm differ by ca 1 log unit, which is close
236 to the maximal error (0.94 log units) found in the model validation presented above. The reason for
237 the model disagreement specifically for 1,2,9,10- $C_{10}Cl_4$ and 1,2,10,11- $C_{10}Cl_4$ is unknown, but we
238 speculate that an extended sequence of non-Cl-substituted $-CH_2-$ units rarely occurs in our random
239 isomer generation for the training set and thus may have been under-represented in the model
240 training. Indeed, our training set contained only two congeners with a $-CH_2-CH_2-CH_2-CH_2-$ fragment
241 and none with a longer CH_2 chain. That said, the experimental K_{aw} value for 1,2,9,10- $C_{10}Cl_4$ could also
242 be somewhat too high, as $\log K_{aw}$ of -2 in combination with $\log K_{ow}$ of 5 would result in $\log K_{oa}$ of 7
243 (via $K_{oa} = K_{ow}/K_{aw}$) and this is even smaller than an experimentally measured log hexadecane–air
244 partition coefficient (L) of 8.4 for 1,2,9,10- $C_{10}Cl_4$.²² $K_{oa} \gtrsim L$ is generally expected because CPs interact
245 with octanol via additional polar interactions that do not occur with apolar hexadecane.



246

247 Figure 2. Comparison of predicted with experimental K values. Predictions were derived from
248 COSMO-RS based FCMs (with PLSR calibration) as well as directly from COSMOtherm software. K_{ow}
249 data are from Hilger et al.²⁴ K_{aw} data are from Drouillard et al.²⁵ for 23°C. There are multiple data
250 points both for predictions and experimental data because of the presence of diastereomers. Bars
251 indicate the mean.

252

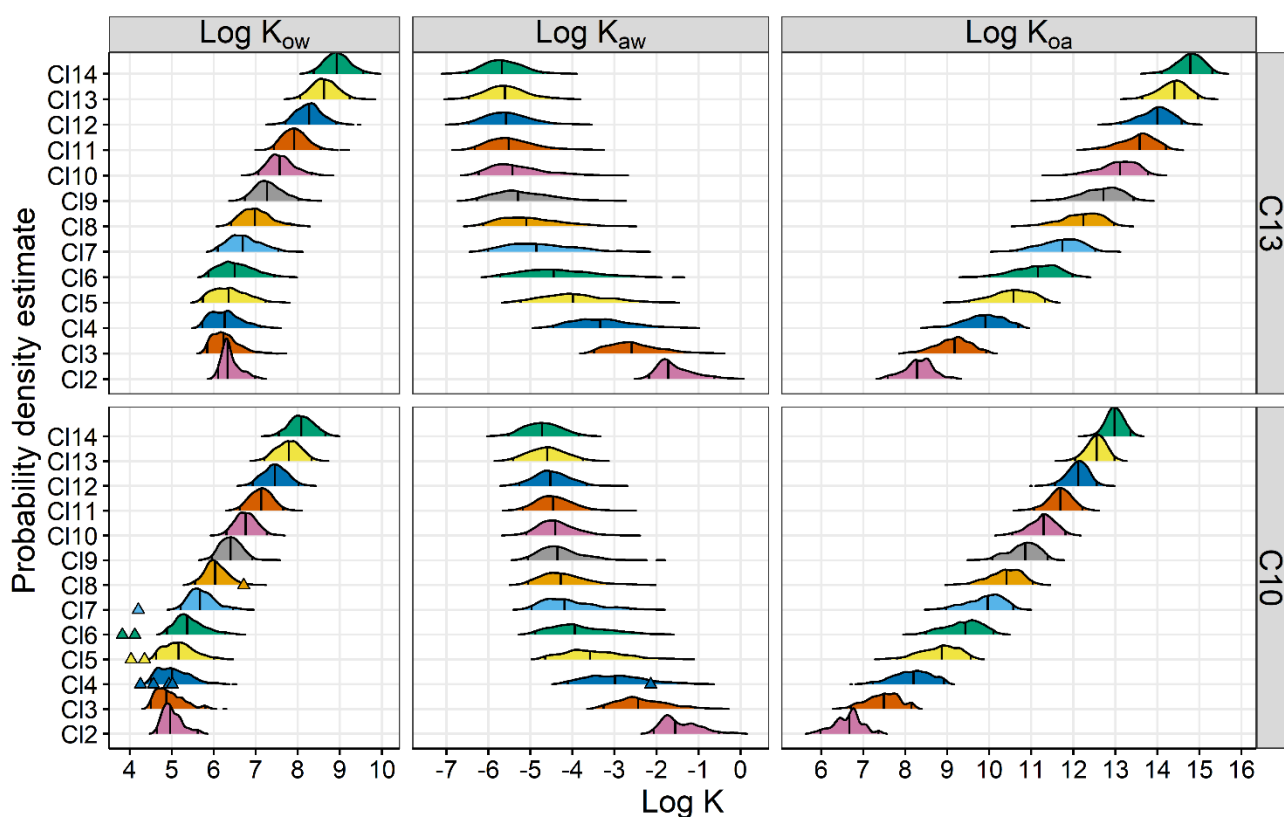
253 **Distributions of K_{ow} , K_{aw} , and K_{oa} for SCCP congener groups.** Using the FCM based on PLSR
254 calibration, log K 's for 1000 isomers per congener group were predicted. These predictions were
255 used to estimate the distributions of K_{ow} , K_{aw} , and K_{oa} for SCCP congener groups (Figures 3, S5; here
256 double/triple Cl is not allowed). The 2.5, 25, 50 (median), 75, and 97.5%iles of log K 's for each SCCP
257 congener group are presented in Tables S5.

258 Log K_{ow} and log K_{oa} for each congener group are within a relatively narrow range (1 to 2 log
259 units), whereas log K_{aw} for each congener group spreads over 1.5 to 3 log units. The median log K_{ow}
260 values of different SCCP congener groups range over 4 log units (5.0 to 8.9) and log K_{aw} also over 4
261 log units (-5.7 to -1.6), whereas the median log K_{oa} spans over 8 log units (6.7 to 14.8).

262 It is interesting that the medians of log K_{ow} , K_{aw} , and K_{oa} show different dependence on the
263 numbers of C and Cl. All three log K 's are linearly dependent on the number of C, although the slopes
264 differ depending on the partitioning phases and partially on the number of Cl (Figure S6). In contrast,
265 dependence on the number of Cl is nonlinear (Figure 3; more clearly in Figure S7). Log K_{ow} is fairly
266 constant from Cl₂ to ~Cl₅, above which it increases with ca 0.35 log units/C. Log K_{aw} has the opposite
267 trend; it decreases from Cl₂ to ~Cl₁₀ by 2.5–3.5 log units and thereafter stays nearly the same. Log K_{oa}
268 monotonically increases but in a concave downward shape. The increase is ca 0.8 log unit/Cl from Cl₂
269 to Cl₃ whereas only 0.4 log units/Cl from C₁₃ to C₁₄.

270 We also derived the distributions of partition coefficients for CP congeners without double
271 and triple Cl substitutions (Figure S8, Table S6). The distribution peaks are sometimes slightly sharper,
272 but overall, the results are just similar to the distributions of CP congeners including double/triple Cl
273 substitutions. The median for each congener group is different by only 0.13 log unit on average and
274 by 0.39 at most. The similarity between the cases with and without double/triple Cl is expected for
275 low-chlorinated congeners (Cl₂–Cl₄), because random generation forms limited numbers of double
276 and triple substitutions, even if allowed. The similarity for higher chlorinated congeners is interesting
277 and suggests that this difference is not important for partition coefficients when the congener groups
278 are considered as a whole.

279



280

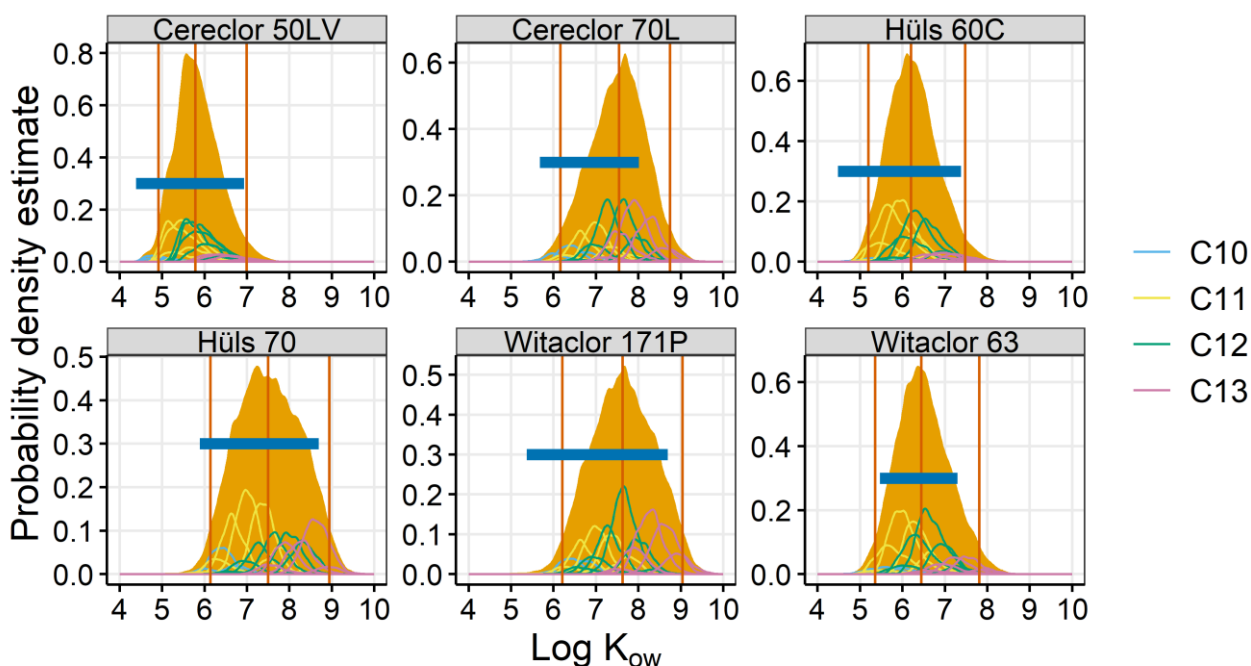
281 Figure 3. Kernel density estimates resulting from 1000 structures (with double and triple Cl
 282 substitution allowed) for each molecular formula (predicted by PLSR model). Vertical lines indicate
 283 the 2.5, 50 (median), and 97.5%iles. Data points are experimental data from Hilger et al.²⁴ and
 284 Drouillard et al.²⁵ for specific isomers. Plots with more congener groups and without double and triple
 285 Cl substitutions are shown in Figures S5 and S8.

286

287 **Predicting log K_{ow} of SCCP mixtures.** The log K_{ow} distributions predicted above for all relevant
 288 SCCP congener groups were used in combination with the compositions of SCCP mixtures
 289 experimentally derived from Yuan et al.²⁶ to predict log K_{ow} ranges of bulk CP mixtures (Figure 4; more
 290 plots in Figures S9, S10). Here, the predicted log K_{ow} distributions for congener groups were weighted
 291 by their relative abundance (i.e., mole fractions) in the mixture and were then summed. The results
 292 agreed with the experimental data from Renberg et al.,²⁷ who used retentions on thin layer
 293 chromatography to estimate the ranges of log K_{ow} for CP mixtures. The lower bound of the
 294 experimental data agrees with the predicted 2.5%ile and the upper bound with the predicted
 295 97.5%ile within 0.84 log units (Table S7). These results serve as additional validation of COSMOtherm
 296 and the FCMs for predicting log K_{ow} of CPs.

297

298



299

300 Figure 4. Comparison of predicted distributions of $\log K_{ow}$ for CP mixtures (filled curves) and
 301 experimental data from Renberg et al.²⁷ (horizontal bars). The 2.5, 50, and 97.5%iles of the
 302 predications for mixtures (vertical lines) and the predictions for each congener groups (unfilled
 303 curves) are also shown. The predictions were derived from the FCMs (PLSR, double/triple CI allowed).

304

305 **Implications.** This study presents, for the first time, a time-efficient method to predict
 306 partition coefficients for a large number of CP congeners on the basis of quantum chemical
 307 calculations. We provided the ranges of partition coefficients for CP congener groups and bulk CP
 308 mixtures, grounded on the predictions for individual congeners. These new pieces of information
 309 should improve our understanding on the environmental fate of CPs. As an example, SCCP congeners
 310 were plotted in the chemical space that indicates the Arctic bioaccumulation potential using
 311 predicted $\log K_{aw}$ and $\log K_{oa}$, following the approach by Czub et al.²⁸ and Brown and Wania²⁹ (Figure
 312 5; plots for each SCCP congener group is shown in Figure S10). Figure 5 shows that relatively low
 313 chlorinated (Cl_2 – Cl_6) SCCPs fall into the chemical space where high Arctic bioaccumulation is expected,
 314 assuming perfect persistence. In contrast, SCCPs with relatively high molecular weight ($C + Cl \geq 20$) do
 315 not fall in this zone. Previously, Gawor and Wania³⁰ presented various chemical space plots for CPs
 316 using $\log K_{aw}$ and $\log K_{oa}$ predicted by ACD/ADME Suite prediction tools and came up with conclusions
 317 that are in part similar to those in this work. It would be interesting to repeat their analysis with the
 318 predicted partition coefficients from this work, which is however beyond the scope of this article.

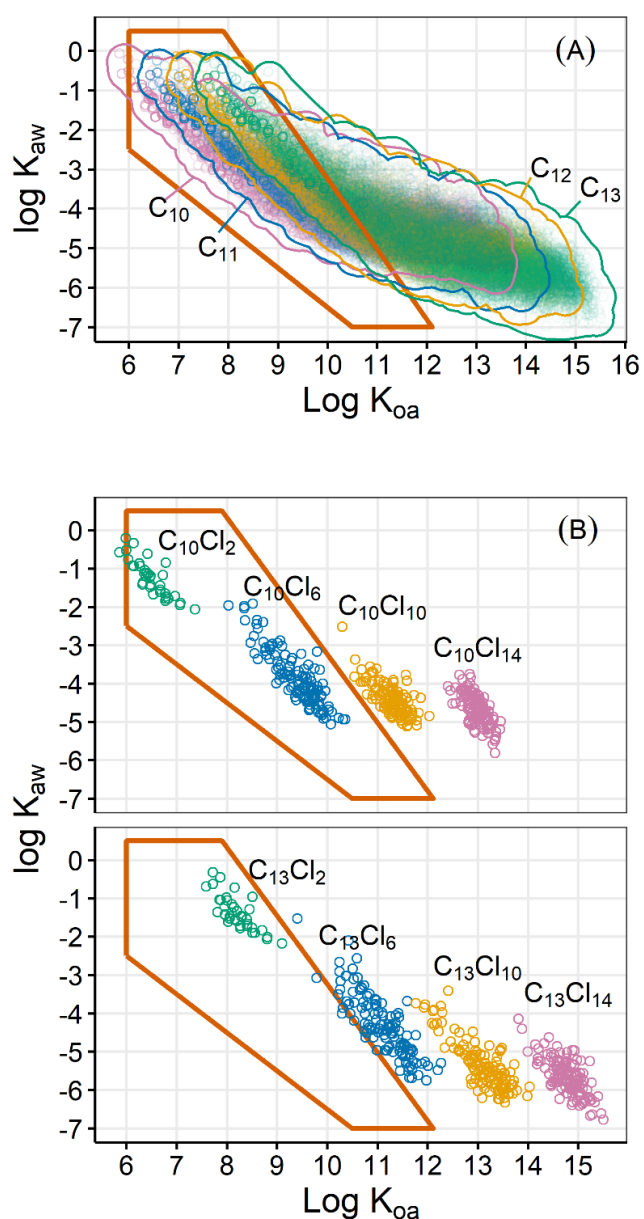
319

320 The presented approach of course has room for further improvement. First, the current FCMs
 321 have been calibrated with relatively short CPs ($\leq C_{10}$) and thus would have to be extrapolated for
 M/LCCPs. Extension to M/LCCPs requires lengthy COSMOconfX calculations for long molecules, which

322 will be conducted as a next step. Second, while the current study demonstrated good model
323 predictions for $\log K_{ow}$ of a dozen of individual constitutional isomers and six bulk SCCP mixtures,
324 validation for more of specific (stereo)isomers and other partition phases would be desirable. This
325 statement applies both to the original COSMO-RS approach and the FCMs presented here. Availability
326 of isomer-specific CP standards is being improved and more data are expected in the future (e.g., ref
327 22). Third, the current work used randomly generated congeners from all Cl substitution patterns or
328 excluding double and triple Cl substitutions to represent the congener composition of each CP
329 congener group, but this is a first approximation. As more and more knowledge regarding Cl
330 substitution patterns in the bulk CP mixtures is becoming available,^{19,23,31} congener compositions
331 used for the prediction of partition coefficients could be elaborated further.

332 This study demonstrated that the approach that combines COSMO-RS and FCM methods can
333 provide accurate predictions for SCCP partitioning coefficients. As the most time-consuming
334 COSMO*confX* step that generates COSMO files has been completed for a number of CP congeners, it
335 is possible to run COSMO*therm* and derive new FCMs quickly for other partition coefficients or other
336 properties of CPs that are related to the chemical potential in solvent. Our approach may be useful
337 for other highly complex mixtures as well, as partitioning properties of complex mixtures are generally
338 difficult to determine both experimentally and computationally.

339



340

341 Figure 5. Chemical space plots for (A) all and (B) selected SCCP congener groups. The chemical space
 342 for a high Arctic contamination and bioaccumulation potential AC-BAP (>10%, 70 days)²⁸ was enclosed
 343 with lines, as in ref 29.

344

345

346 [Associated Content](#)

347 Supporting Information

348

349 Additional figures and tables for the results of model fitting and validation, model predictions
 350 for log K 's, distributions of log K_{ow} , and chemical space plots. This material is available free of charge
 351 via the Internet at <http://pubs.acs.org>.

351

352 Author Information

353 Corresponding author

354 Satoshi Endo

355 Phone/Fax: ++81-29-850-2695

356 endo.satoshi@nies.go.jp

357 ORCID: 0000-0001-8702-1602

358

359 Notes

360 The authors declare no competing financial interest.

361

362 Author contributions

363 Study design: SE. COSMO-RS calculations: SE, JH. Statistical analysis: SE. Data evaluation: SE.

364 Drafting of manuscript: SE. Revising of manuscript: SE, JH.

365

366 Acknowledgements

367 We thank Frank Wania, Trevor Brown, and Kai-Uwe Goss for their valuable comments on the
368 manuscript. COSMOconfX and TURBOMOL calculations were performed with the NIES
369 supercomputer system. This work was supported by the Environment Research and Technology
370 Development Fund (SII-3-1) of the Environmental Restoration and Conservation Agency, Japan.

371

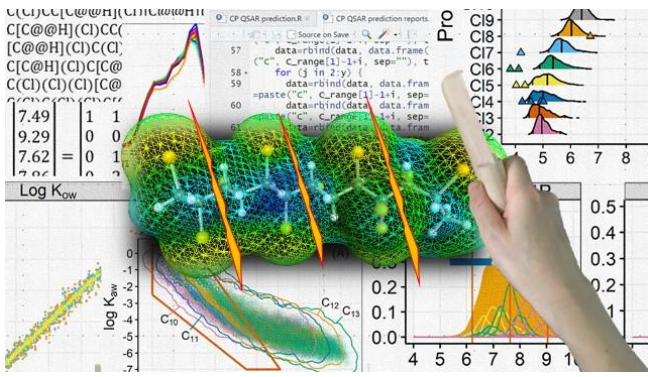
372 References

- 373 1. UNEP, Decision SC-8/11: Listing of short-chain chlorinated paraffins. 2017,
374 UNEP/POPS/COP.8/SC-8/11.
- 375 2. Glüge, J.; Schinkel, L.; Hungerbühler, K.; Cariou, R.; Bogdal, C., Environmental risks of
376 medium-chain chlorinated paraffins (MCCPs): A Review. *Environ. Sci. Technol.* **2018**, *52*, (12),
377 6743-6760.
- 378 3. van Mourik, L. M.; Lava, R.; O'Brien, J.; Leonards, P. E. G.; de Boer, J.; Ricci, M., The
379 underlying challenges that arise when analysing short-chain chlorinated paraffins in
380 environmental matrices. *J. Chromatogr. A* **2020**, *1610*, 460550.
- 381 4. Korytar, P.; Parera, J.; Leonards, P. E.; Santos, F. J.; de Boer, J.; Brinkman, U. A.,
382 Characterization of polychlorinated *n*-alkanes using comprehensive two-dimensional gas
383 chromatography--electron-capture negative ionisation time-of-flight mass spectrometry. *J.*
384 *Chromatogr. A* **2005**, *1086*, (1-2), 71-82.
- 385 5. Klamt, A., Conductor-like screening model for real solvents: A new approach to the
386 quantitative calculation of solvation phenomena. *J. Phys. Chem.* **1995**, *99*, (7), 2224-2235.
- 387 6. Stenzel, A.; Goss, K.-U.; Endo, S., Prediction of partition coefficients for complex
388 environmental contaminants: Validation of COSMOtherm, ABSOLV, and SPARC. *Environ.*
389 *Toxicol. Chem.* **2014**, *33*, (7), 1537-1543.

- 390 7. Loschen, C.; Reinisch, J.; Klamt, A., COSMO-RS based predictions for the SAMPL6 logP
391 challenge. *J. Comput. Aided Mol. Des.* **2020**, *34*, (4), 385-392.
- 392 8. Goss, K.-U.; Arp, H. P. H.; Bronner, G.; Niederer, C., Partition behavior of
393 hexachlorocyclohexane isomers. *J. Chem. Eng. Data* **2008**, *53*, (3), 750-754.
- 394 9. Glüge, J.; Bogdal, C.; Scheringer, M.; Buser, A. M.; Hungerbühler, K., Calculation of
395 physicochemical properties for short- and medium-chain chlorinated paraffins. *J. Phys.*
396 *Chem. Ref. Data* **2013**, *42*, (2), 023103.
- 397 10. Meylan, W. M.; Howard, P. H., Atom/fragment contribution method for estimating octanol-
398 water partition coefficients. *J. Pharm. Sci.* **1995**, *84*, (1), 83-92.
- 399 11. Brown, T. N.; Arnot, J. A.; Wania, F., Iterative fragment selection: a group contribution
400 approach to predicting fish biotransformation half-lives. *Environ. Sci. Technol.* **2012**, *46*, (15),
401 8253-8260.
- 402 12. OECD, Guidance document on the validation of (quantitative) structure-activity relationships
403 [(Q)SAR] models. 2007, ENV/JM/MONO(2007)2.
- 404 13. Dearden, J. C.; Cronin, M. T.; Kaiser, K. L., How not to develop a quantitative structure-activity
405 or structure-property relationship (QSAR/QSPR). *SAR QSAR Environ. Res.* **2009**, *20*, (3-4),
406 241-266.
- 407 14. Ramakrishnan, R.; von Lilienfeld, O. A., Machine learning, quantum chemistry, and chemical
408 space. In *Reviews in Computational Chemistry, Vol 30*, Parrill, A. L.; Lipkowitz, K. B., Eds.
409 Wiley-Blackwell: Malden, 2017; Vol. 30, pp 225-256.
- 410 15. R Core Team, *R: A language and environment for statistical computing*. R Foundation for
411 Statistical Computing, Vienna, Austria. <https://www.R-project.org/>. 2019.
- 412 16. O'Boyle, N. M.; Banck, M.; James, C. A.; Morley, C.; Vandermeersch, T.; Hutchison, G. R.,
413 Open Babel: An open chemical toolbox. *J. Cheminformatics* **2011**, *3*, (1), 33.
- 414 17. Cao, Y.; Charisi, A.; Cheng, L. C.; Jiang, T.; Girke, T., ChemmineR: a compound mining
415 framework for R. *Bioinformatics* **2008**, *24*, (15), 1733-1734.
- 416 18. Burnham, K. P.; Anderson, D. R., Multimodel Inference. *Sociol. Methods Res.* **2016**, *33*, (2),
417 261-304.
- 418 19. Yuan, B.; Lysak, D. H.; Soong, R.; Haddad, A.; Hisatsune, A.; Moser, A.; Golotvin, S.;
419 Argyropoulos, D.; Simpson, A. J.; Muir, D. C. G., Chlorines are not evenly substituted in
420 chlorinated paraffins: A predicted nmr pattern matching framework for isomeric
421 discrimination in complex contaminant mixtures. *Environ. Sci. Technol. Letters* **2020**.
422 doi.org/10.1021/acs.estlett.0c00244.
- 423 20. Fredricks, P. S.; Tedder, J. M., 28. Free-radical substitution in aliphatic compounds. Part II.
424 Halogenation of the *n*-butyl halides. *J. Chem. Soc. (Resumed)* **1960**, 144-150.
- 425 21. Colebourne, N.; Stern, E. S., 660. The chlorination of some *n*-alkanes and alkyl chlorides. *J.*
426 *Chem. Soc. (Resumed)* **1965**, 3599-3605.
- 427 22. Hammer, J.; Matsukami, H.; Endo, S., Congener-specific partition properties of chlorinated

- 428 paraffins evaluated with COSMOtherm and GC-retention indices. (Manuscript in
429 preparation).
- 430 23. Sprengel, J.; Wiedmaier-Czerny, N.; Vetter, W., Characterization of single chain length
431 chlorinated paraffin mixtures with nuclear magnetic resonance spectroscopy (NMR).
432 *Chemosphere* **2019**, *228*, 762-768.
- 433 24. Hilger, B.; Fromme, H.; Volkel, W.; Coelhan, M., Effects of chain length, chlorination degree,
434 and structure on the octanol-water partition coefficients of polychlorinated *n*-alkanes.
435 *Environ Sci Technol* **2011**, *45*, (7), 2842-9.
- 436 25. Drouillard, K. G.; Tomy, G. T.; Muir, D. C. G.; Friesen, K. J., Volatility of chlorinated n-alkanes
437 (C-10-C-12): Vapor pressures and Henry's law constants. *Environ. Toxicol. Chem.* **1998**, *17*,
438 (7), 1252-1260.
- 439 26. Yuan, B.; Bogdal, C.; Berger, U.; MacLeod, M.; Gebbink, W. A.; Alsberg, T.; de Wit, C. A.,
440 Quantifying short-chain chlorinated paraffin congener groups. *Environ. Sci. Technol.* **2017**,
441 *51*, (18), 10633-10641.
- 442 27. Renberg, L.; Sundstrom, G.; Sundhnygard, K., Partition coefficients of organic chemicals
443 derived from reversed phase thin-layer chromatography: Evaluation of methods and
444 application on phosphate esters, polychlorinated paraffins and some PCB-substitutes.
445 *Chemosphere* **1980**, *9*, (11), 683-691.
- 446 28. Czub, G.; Wania, F.; McLachlan, M. S., Combining long-range transport and bioaccumulation
447 considerations to identify potential Arctic contaminants. *Environ. Sci. Technol.* **2008**, *42*, (10),
448 3704-3709.
- 449 29. Brown, T. N.; Wania, F., Screening chemicals for the potential to be persistent organic
450 pollutants: A case study of Arctic contaminants. *Environ. Sci. Technol.* **2008**, *42*, (14), 5202-
451 5209.
- 452 30. Gawor, A.; Wania, F., Using quantitative structural property relationships, chemical fate
453 models, and the chemical partitioning space to investigate the potential for long range
454 transport and bioaccumulation of complex halogenated chemical mixtures. *Environ. Sci.*
455 *Process Impacts* **2013**, *15*, (9), 1671-1684.
- 456 31. Jensen, S. R.; Brown, W. A.; Heath, E.; Cooper, D. G., Characterization of polychlorinated
457 alkane mixtures-A Monte Carlo modeling approach. *Biodegradation* **2007**, *18*, (6), 703-717.
- 458
- 459

460 TOC



461

462